Effect of resonator dimensions on nonlinear standing waves

C. Luo, X. Y. Huang, and N. T. Nguyen
School of Mechanical and Production Engineering, Nanyang Technological University, Singapore 639798

(Received 13 May 2004; revised 7 October 2004; accepted 9 October 2004)

An investigation of the effect of resonator dimensions on nonlinear standing waves in shaped resonators is conducted. Simple forms of the shear viscosity term in the momentum equations are developed for an axisymmetric (2D) resonator and a low aspect ratio rectangular (3D) resonator. The cross sections of the resonators are exponentially expanded and the one-dimensional wave equations are solved by using the Galerkin's method. The quality factors, pressure waveforms, compression ratios, and resonance frequencies are calculated for different dimensionless cross sections and lengths of the resonators. The results show that, apart from the resonator length, the ratio of the cross-section dimension to the length of the resonator is an important parameter. If the ratio is greater than 0.04, the characteristics of the shaped resonator are not affected significantly. However, when the ratio is less than 0.01, the resonance becomes weak, the compression ratio drops substantially, and the frequency response changes as well.
[DOI: 10.1121/1.1828611]

PACS numbers: 43.25.Gf, 43.20.Hq [MFH] Pages: 96–103

I. INTRODUCTION

The generation of high-amplitude pressure oscillations has recently been achieved, both in experiment[1] and in theoretical modelings,[2–5] in shaped resonators. In contrast to a normal cylindrical resonator, the higher-order modal frequencies in the shaped resonators are no longer multiples of the fundamental frequency, so that the energy transfer from the fundamental frequency to the higher harmonics is less efficient and the large-amplitude pressures are therefore generated. Lawrenson *et al.*[1] conducted experiments by shaking shaped resonators, and standing wave overpressures in excess of 340% ambient pressure were recorded. Ilinskii *et al.*[2] developed a one-dimensional model to analyze the nonlinear standing waves in shaped resonators. The large-amplitude pressures, waveform distortion, and resonance frequency shift were calculated and compared with the experimental results. The one-dimensional model was later improved by including the shear viscosity term in the momentum equation,[3] and the energy losses and quality factors were evaluated. An analytical study was conducted by Hamilton *et al.*[4] to predict and explain the dependence of the nonlinear frequency response on resonator shapes. Most recently, Erickson and Zinn[5] proposed a procedure to solve the one-dimensional wave equation for an exponentially shaped resonator by the Galerkin method. The compression ratio of the maximum to minimum pressures was calculated for different flare constants.

The large-amplitude pressure waves may have applications in miniature- or microscale fluid mechanics, known as microfluidics. This is currently an active research field[6,7] driven by fast development in biomedical engineering and life science. In the microfluidics, conventional fluid devices are shrunk in size to control and deliver fluid in miniature- or microscales. The applications of nonlinear acoustics in microfluidics have been seen, for example, in acoustic streaming[8] for liquid fluid manipulation in microchannels and in miniature synthetic jets[9] for aerodynamics control. The generation of high-pressure gas in micro- or miniature scales is probably more difficult than pumping liquids in microchannels, and it would be interesting to see if this can be achieved by the shaped acoustic resonators. The results may be used to develop miniature- or microcompressors, which are important in microscale cooling technologies and other bioengineering applications. This motivates the present study. The purpose of this study is to investigate how the nonlinear pressure waves change in a shaped acoustic resonator when the overall dimension of the resonator is shrunk, especially when the cross section is reduced. It is known that the resonance frequencies are determined primarily by lengths of the resonators, also by the shape variations in the axial direction. The cross sections of the resonators, on the other hand, affect the acoustical field through the shear viscosity. With a full recognition of the comprehensive work on energy losses conducted by Ilinskii *et al.*,[3] we develop in the present article a simple form for the shear viscosity term, so that the effect of the size reduction may be evaluated easily. The one-dimensional wave equation is then solved by the Galerkin method[5] for two kinds of shaped resonators. One is an exponentially expanded horn with axisymmetric cross sections, in which the acoustic field is two-dimensional (2D). The length of the resonator is l and radius at the small end is r_0. The other is an exponentially expanded horn with low aspect ratio rectangular cross sections, which would be easily fabricated with micromachine technologies. The acoustic field in this low aspect ratio rectangular resonator is essentially three-dimensional (3D). The height of the rectangular cross section is fixed at h and is much smaller than the width b for the most part, and the dynamics of the gas inside the horn can be considered as quasi-two-dimensional. The low aspect ratio rectangular resonator is referred as the 3D resonator in this paper to distinguish it from the axisymmetric resonator, which is referred as the 2D resonator. The quality factors, dynamic pressure waveforms, compression ratios, and resonance frequencies are calculated for different values

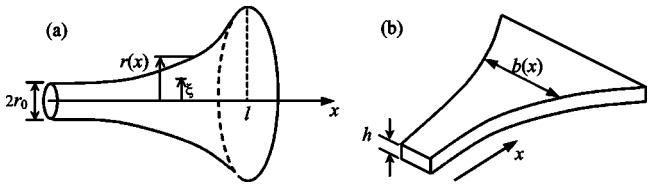

FIG. 1. Geometry and coordinates of the horn-shaped resonators. (a) 2D resonator, and (b) 3D resonator.

of r_0/l and h/l ranging from 0.01 to 0.1, in which the shear viscosity may play an important role in affecting the characteristics of shaped resonators.

II. SHEAR VISCOSITY TERMS AND WAVE EQUATIONS

A. Basic equations

We consider the one-dimensional acoustic wave field in a 2D resonator driven by an acceleration $a(t)$ along the axial direction, as shown in Fig. 1(a). The resonator is closed at both ends and the cross section is expanded in the x direction. The axial velocity along the x direction is $u=u(x,\xi,t)$, depending on x, t, and the radial location ξ. The velocity is not uniform over the cross section of the resonator, especially $u(x,\xi,t)=0$ on the wall of the resonator. The average velocity of u over the cross section can be calculated by

$$\overline{u}(x,t)=\frac{1}{\pi r^2}\int_0^r 2\pi u(x,\xi,t)\xi\, d\xi, \tag{1}$$

and the mass flux through the cross section is therefore

$$F=\int_0^r 2\pi\rho u(x,\xi,t)\xi\, d\xi=\rho\overline{u}\pi r^2. \tag{2}$$

It can be deduced, according to Eq. (2), that the velocity u in the continuity equation and momentum equation developed by Ilinskii *et al.*[2] was actually the average velocity $\overline{u}(x,t)$, and these equations can be rewritten as

$$\frac{\partial\rho}{\partial t}+\frac{1}{r^2}\frac{\partial}{\partial x}(r^2\rho\overline{u})=0, \tag{3}$$

$$\frac{\partial\overline{u}}{\partial t}+\underline{u}\frac{\partial\overline{u}}{\partial x}=-\frac{1}{\rho}\frac{\partial p}{\partial x}-a(t)+\frac{(\zeta+4\eta/3)}{\rho}\frac{\partial}{\partial x}\left(\frac{1}{r^2}\frac{\partial}{\partial x}(r^2\overline{u})\right), \tag{4}$$

where p is the pressure, $a(t)$ is the acceleration of the resonator, and ζ and η are coefficients of bulk and shear viscosities, respectively. We show in the following that the dissipative term in Eq. (4) can be derived from the viscous stress, together with an additional shear viscosity term. The general dissipative term used by Ilinskii *et al.*[2] can be expressed as[10]

$$\eta\frac{\partial^2 u_i}{\partial x_k\partial x_k}+\left(\zeta+\frac{1}{3}\eta\right)\frac{\partial^2 u_k}{\partial x_i\partial x_k}=\eta(\nabla^2\mathbf{u})_i+\left(\zeta+\frac{1}{3}\eta\right)[\nabla(\nabla\cdot\mathbf{u})]_i=\eta\{(\nabla^2\mathbf{u})_i-[\nabla(\nabla\cdot\mathbf{u})]_i\}+\left(\zeta+\frac{4}{3}\eta\right)[\nabla(\nabla\cdot\mathbf{u})]_i. \tag{5}$$

Let i in Eq. (5) be the x component of the velocity vector $\mathbf{u}$; the second term on the right-hand side becomes

$$\left(\zeta+\frac{4}{3}\eta\right)[\nabla(\nabla\cdot\mathbf{u})]_i=\left(\zeta+\frac{4}{3}\eta\right)\frac{\partial}{\partial x}(\nabla\cdot\mathbf{u}). \tag{6}$$

By taking average velocity over the cross section and using the continuity equation (3) for $\nabla\cdot\mathbf{u}$, one obtains the dissipative term in Eq. (4), which is the viscosity term associated with the volume expansion of the gas and was derived by Ilinskii *et al.*[2] The first term on the right-hand side of Eq. (5) is expressed in the cylindrical coordinates (x,ξ,θ) for the 2D resonator, and for the x component of the velocity it becomes

$$\eta\{(\nabla^2\mathbf{u})_i-[\nabla(\nabla\cdot\mathbf{u})]_i\}=\eta\frac{1}{\xi}\frac{\partial}{\partial\xi}\left(\xi\frac{\partial u}{\partial\xi}\right). \tag{7}$$

Equation (7) is a term induced by the shear motion of the velocity and is referred as the shear viscosity term. The evaluation of this term and its average depends on the velocity profile over the cross section, i.e., $u(x,\xi,t)$. By including the average of Eq. (7) in Eq. (4), one obtains

$$\frac{\partial\overline{u}}{\partial t}+\underline{u}\frac{\partial\overline{u}}{\partial x}=-\frac{1}{\rho}\frac{\partial p}{\partial x}-a(t)+\frac{(\zeta+4\eta/3)}{\rho}\frac{\partial}{\partial x}\times\left(\frac{1}{r^2}\frac{\partial}{\partial x}(r^2\overline{u})\right)+\frac{\eta}{\rho}\overline{\frac{1}{\xi}\frac{\partial}{\partial\xi}\left(\xi\frac{\partial u}{\partial\xi}\right)}. \tag{8}$$

A similar procedure has been applied to the 3D resonator, shown in Fig. 1(b), in a Cartesian coordinate system, and Eqs. (3) and (4) are modified as

$$\frac{\partial\rho}{\partial t}+\frac{1}{hb}\frac{\partial}{\partial x}(hb\rho\overline{u})=0, \tag{9}$$

$$\frac{\partial\overline{u}}{\partial t}+\underline{u}\frac{\partial\overline{u}}{\partial x}=-\frac{1}{\rho}\frac{\partial p}{\partial x}-a(t)+\frac{(\zeta+4\eta/3)}{\rho}\frac{\partial}{\partial x}\times\left(\frac{1}{hb}\frac{\partial}{\partial x}(hb\overline{u})\right)+\frac{\eta}{\rho}\overline{\frac{\partial^2 u}{\partial\xi^2}}. \tag{10}$$

In Eq. (10), $\eta\overline{\partial^2 u/\partial\xi^2}$ is the shear viscosity term, and the evaluation of this term depends also on the velocity profile over the duct cross section. The shear viscosity terms in both Eqs. (8) and (10) are derived in the next section.

B. Velocity profiles and shear viscosity terms

For the 2D resonator, we consider a tube with a circular cross section of radius r; the linear equation associated with the shear viscosity is

$$\rho\frac{\partial u}{\partial t}=-\frac{\partial p}{\partial x}+\eta\frac{1}{\xi}\frac{\partial}{\partial\xi}\left(\xi\frac{\partial u}{\partial\xi}\right). \tag{11}$$

By setting $u=v(x,\xi)e^{i\omega t}$, $\partial p/\partial x=p_x e^{i\omega t}$ (the real part will be taken from the results), and substituting them into Eq. (11), one obtains

$$\frac{\partial^2 v}{\partial \xi^2}+\frac{1}{\xi}\frac{\partial v}{\partial \xi}+\beta^2 v=\frac{p_x}{\eta}, \tag{12}$$

where $\beta^2=-(i\rho\omega/\eta)$, and $\beta=(1-i)\sqrt{\rho\omega/2\eta}$. The solution of Eq. (12), subject to boundary condition $v|_{\xi=r}=0$ and v being finite at $\xi=0$, is

$$v=\frac{p_x}{\eta\beta^2}\left[1-\frac{J_0(\beta\xi)}{J_0(\beta r)}\right].\ \text{Thus,}$$

$$u=ve^{i\omega t}=U(x,t)\left[1-\frac{J_0(\beta\xi)}{J_0(\beta r)}\right], \tag{13}$$

where $U(x,t)=p_x e^{i\omega t}/\eta\beta^2$. The average of u over the cross section of the tube is

$$\overline{u}=\frac{U(x,t)}{\pi r^2}\int_0^r 2\pi\xi\left[1-\frac{J_0(\beta\xi)}{J_0(\beta r)}\right]d\xi$$

$$=U(x,t)\left[1-\frac{2J_1(\beta r)}{\beta r J_0(\beta r)}\right]. \tag{14}$$

Using the velocity profile (13), the shear viscosity term in the momentum equation can be evaluated as

$$\eta\frac{1}{\xi}\frac{\partial}{\partial\xi}\left(\xi\frac{\partial u}{\partial\xi}\right)=U(x,t)\frac{\eta\beta^2}{J_0(\beta r)}J_0(\beta\xi). \tag{15}$$

The average of the shear viscosity term (15) over the tube cross section is

$$\overline{\eta\frac{1}{\xi}\frac{\partial}{\partial r}\left(\xi\frac{\partial u}{\partial\xi}\right)}=U(x,t)\frac{\eta\beta^2}{J_0(\beta r)}\frac{1}{\pi r^2}\int_0^r 2\pi\xi J_0(\beta\xi)d\xi$$

$$=U(x,t)\frac{2\eta\beta}{r}\frac{J_1(\beta r)}{J_0(\beta r)}$$

$$=\frac{2\eta\beta}{r}\frac{J_1(\beta r)}{J_0(\beta r)}\left[1-\frac{2J_1(\beta r)}{(\beta r)J_0(\beta r)}\right]^{-1}\overline{u}, \tag{16}$$

in which Eq. (14) has been used to eliminate $U(x,t)$. It can be shown[11] that for $|\beta r|\gg 1$, $J_1(\beta r)/J_0(\beta r)\to -i$; therefore

$$\overline{\eta\frac{1}{\xi}\frac{\partial}{\partial r}\left(\xi\frac{\partial u}{\partial\xi}\right)}\xrightarrow{|\beta r|\gg 1}\frac{2\eta\beta}{r}(-i)\left[1+\frac{2i}{(\beta r)}\right]^{-1}\overline{u}$$

$$\simeq(-1-i)\frac{\sqrt{2\eta\rho\omega}}{r}\overline{u}. \tag{17}$$

By taking the real part of Eq. (17), we have

$$\overline{\eta\frac{1}{\xi}\frac{\partial}{\partial r}\left(\xi\frac{\partial u}{\partial\xi}\right)}\xrightarrow{|\beta r|\gg 1}-\frac{\sqrt{2\eta\rho\omega}}{r}\overline{u}. \tag{18}$$

For the 3D resonator, we consider a two-dimensional duct; Eqs. (11) and (12) in this case become

$$\rho\frac{\partial u}{\partial t}=-\frac{\partial p}{\partial x}+\eta\frac{\partial^2 u}{\partial\xi^2}, \tag{19}$$

$$\frac{\partial^2 v}{\partial\xi^2}-\beta^2 v=\frac{p_x}{\eta}, \tag{20}$$

where $\beta^2=i\rho\omega/\eta$, and $\beta=(1+i)\sqrt{\rho\omega/2\eta}$. The velocity u obtained from the solution of Eq. (20), subject to boundary conditions $v|_{\xi=h}=v|_{\xi=0}=0$, is

$$u=ve^{i\omega t}=U(x,t)\left\{\cosh(\beta y)-1-\frac{\cosh(\beta h)-1}{\sinh(\beta h)}\sinh(\beta y)\right\}, \tag{21}$$

where $U(x,t)=p_x e^{i\omega t}/\eta\beta^2$. The average of u over the duct height is

$$\overline{u}=\frac{U(x,t)}{\beta h}\left\{\sinh(\beta h)-\beta h-\frac{[\cosh(\beta h)-1]^2}{\sinh(\beta h)}\right\}. \tag{22}$$

The average of shear stress $\eta\overline{\partial^2 u/\partial\xi^2}$ can be worked out based on Eq. (21). By following the same procedure for the tube, we have

$$\eta\overline{\frac{\partial^2 u}{\partial\xi^2}}\xrightarrow{|\beta h|\gg 1}-\frac{\sqrt{2\eta\rho\omega}}{h}\overline{u}. \tag{23}$$

The condition $|\beta r|\gg 1$ used in Eqs. (18) and (23) can be justified by taking η in order of 10^{-5}, ω in order of 10^3 (assuming the oscillation frequency to be 500 Hz), so that $|\beta r|\sim r\sqrt{\rho\omega/\eta}\sim r\times 10^4$. The condition $|\beta r|\gg 1$ is therefore equivalent to $|\beta r|\sim r\times 10^4\gg 1$, or, $r\gg 10^{-4}$ m$=0.1$ mm, which can always be met in the present study. Equations (18) and (23) are the shear viscosity terms to be included in the momentum equation for $\overline{u}$. They are equivalent to the term introduced by Ilinskii *et al.*[3] but in simpler forms. It should be pointed out, however, that the dissipations in the work by Ilinskii *et al.*[3] include the turbulence induced energy loss and therefore are more comprehensive when the pressure amplitudes are large.

C. Dimensionless wave equations

With the shear viscosity term expressed in Eq. (18), the momentum equation (8) for the 2D resonator can now be written as

$$\frac{\partial\overline{u}}{\partial t}+\overline{u}\frac{\partial\overline{u}}{\partial x}=-\frac{1}{\rho}\frac{\partial p}{\partial x}-a(t)$$

$$+\frac{(\zeta+4\eta/3)}{\rho}\frac{\partial}{\partial x}\left(\frac{1}{r^2}\frac{\partial}{\partial x}(r^2\overline{u})\right)$$

$$-\frac{\sqrt{2\rho_0\eta\omega}}{r_\rho}\overline{u}. \tag{24}$$

It can be seen from Eq. (24) that the shear viscosity term takes into account the effect of frequency ω and dimension r. The dissipation increases as ω increases and r decreases. By introducing the velocity potential

$$\overline{u}=\frac{\partial\varphi}{\partial x}, \tag{25}$$

and following the same procedure developed by Ilinskii *et al.*[2] and Erickson and Zinn,[4] the dimensionless wave equation becomes

$$\frac{1}{\pi^2 S}\frac{\partial}{\partial X}\left(S\frac{\partial \Phi}{\partial X}\right)-\Omega^2\frac{\partial^2\Phi}{\partial T^2}+\frac{G_B\Omega}{\pi^3 S}\frac{\partial^2}{\partial T\partial X}\times\left(S\frac{\partial\Phi}{\partial X}\right)-\frac{G_S\Omega^{3/2}}{R}\frac{\partial\Phi}{\partial T}=\Omega\frac{\partial A}{\partial T}X+A(T)\frac{\partial\Phi}{\partial X}+\frac{\gamma-1}{S}A(T)X\frac{\partial}{\partial X}\left(S\frac{\partial\Phi}{\partial X}\right)+2\Omega\frac{\partial^2\Phi}{\partial X\partial T}\frac{\partial\Phi}{\partial X}+\frac{(\gamma-1)\Omega}{S}\frac{\partial\Phi}{\partial T}\frac{\partial}{\partial X}\left(S\frac{\partial\Phi}{\partial X}\right)+\frac{\gamma-1}{2S}\left(\frac{\partial\Phi}{\partial X}\right)^2\frac{\partial}{\partial X}\left(S\frac{\partial\Phi}{\partial X}\right). \tag{26}$$

The dimensionless variables are

$$X=\frac{x}{l},\quad T=\omega t,\quad S=\frac{\pi r^2}{l^2},\quad R=\frac{r}{l},\quad A=\frac{a}{l\omega_0^2},$$

$$\Phi=\frac{\varphi}{l^2\omega_0},\quad \Omega=\frac{\omega}{\omega_0}. \tag{27}$$

$$G_B=\frac{\pi\delta\omega_0}{c_0^2},\quad \delta=\frac{\zeta+4\eta/3}{\rho_0},\quad G_S=\sqrt{\frac{2\eta}{\pi\rho_0 c_0 l}},$$

$$\omega_0=\frac{\pi c_0}{l}. \tag{28}$$

Here, G_B is the same as G and D introduced by Ilinskii *et al.*[2] and Erickson and Zinn,[4] respectively, G_S is a parameter associated with the shear viscosity, l is length of the resonator, and c_0 is the speed of sound. Equation (26) shows that the coefficient of the shear viscosity term is inversely proportional to the dimensionless cross-section size, R, and the square root of the resonator length, $\sqrt{l}$.

Similarly, by substituting Eq. (23) into Eq. (10), we obtain the momentum equation for the 3D resonator

$$\frac{\partial\overline{u}}{\partial t}+\overline{u}\frac{\partial\overline{u}}{\partial x}=-\frac{1}{\rho}\frac{\partial p}{\partial x}-a(t)+\frac{(\zeta+4\eta/3)}{\rho}\frac{\partial}{\partial x}\left(\frac{1}{hb}\frac{\partial}{\partial x}(hb\overline{u})\right)-\frac{\sqrt{2\rho_0\eta\omega}}{h}\overline{u}, \tag{29}$$

and the dimensionless wave equation

$$\frac{1}{\pi^2 B}\frac{\partial}{\partial X}\left(B\frac{\partial \Phi}{\partial X}\right)-\Omega^2\frac{\partial^2\Phi}{\partial T^2}+\frac{G_B\Omega}{\pi^3 B}\frac{\partial^2}{\partial T\partial X}\times\left(B\frac{\partial\Phi}{\partial X}\right)-\frac{G_S\Omega^{3/2}}{H}\frac{\partial\Phi}{\partial T}=\Omega\frac{\partial A}{\partial T}X+A(T)\frac{\partial\Phi}{\partial X}+\frac{\gamma-1}{B}A(T)X\frac{\partial}{\partial X}\left(B\frac{\partial\Phi}{\partial X}\right)+2\Omega\frac{\partial^2\Phi}{\partial X\partial T}\frac{\partial\Phi}{\partial X}+\frac{(\gamma-1)\Omega}{B}\frac{\partial\Phi}{\partial T}\frac{\partial}{\partial X}\left(B\frac{\partial\Phi}{\partial X}\right)+\frac{\gamma-1}{2B}\left(\frac{\partial\Phi}{\partial X}\right)^2\frac{\partial}{\partial X}\left(B\frac{\partial\Phi}{\partial X}\right), \tag{30}$$

where $H=h/l$ and $B=[b(x)]/l$, and other parameters are the same as those in Eqs. (27) and (28). It has been assumed that the shear viscosity is important only on upper and lower walls in the 3D resonator.

III. EFFECT OF RESONATOR DIMENSIONS

A. Quality factors

The energy loss in a dynamic system may be measured by quality factors, which is the ratio of total energy stored in the system to the energy dissipated in one cycle. There are many ways to calculate the quality factor and one of them is to use the decay factor, κ, from the time factor $e^{-\kappa t}$, and the quality factor is obtained by[12]

$$Q=\frac{\pi f_0}{\kappa}, \tag{31}$$

where f_0 is the fundamental frequency of the system. Equation (26) can be reduced to a linear equation by dropping all quadratic terms and the driving force A

$$\frac{\partial^2\Phi}{\partial T^2}-\frac{1}{\Omega^2\pi^2}\frac{\partial^2\Phi}{\partial X^2}=\frac{G_B}{\Omega\pi^3}\frac{\partial^3\Phi}{\partial T\partial X^2}-\frac{G_S}{\Omega^{1/2}R}\frac{\partial\Phi}{\partial T}. \tag{32}$$

By substituting the fundamental mode $\Phi=A\cos(\pi X)e^{(i-\sigma)T}=A\cos(\pi X)e^{(i-\sigma)\omega t}$ into Eq. (32), where $\sigma=\kappa/\omega_0$ is the dimensionless decay factor, taking $\Omega=1$ ($\omega=\omega_0$), at which the energy losses are the maximum,[3] and keeping terms of the first order of σ, one obtains

$$\sigma=\frac{1}{2}\left(\frac{G_B}{\pi}+\frac{G_S}{R}\right). \tag{33}$$

In Eq. (33), R follows the resonator expansion profile $R(X)=(r_0/l)f(X)$. By denoting

$$K=\int_0^1\frac{dX}{f(X)}, \tag{34}$$

the average of σ over the resonator length can be calculated as

$$\overline{\sigma}=\frac{1}{2}\left(\frac{G_B}{\pi}+\frac{G_S}{r_0/l}\int_0^1\frac{dX}{f(X)}\right)=\frac{1}{2}\left(\frac{G_B}{\pi}+\frac{KG_S}{r_0/l}\right). \tag{35}$$

The quality factor is calculated by

$$Q=\frac{\pi f_0}{k}=\frac{\pi f_0}{\overline{\sigma}\omega_0}=\left(\frac{G_B}{\pi}+\frac{KG_S}{r_0/l}\right)^{-1}=\left(\frac{1}{Q_B}+\frac{1}{Q_S}\right)^{-1}, \tag{36}$$

where

$$Q_B=\frac{\pi}{G_B}=\frac{c_0\rho_0 l}{\pi(\zeta+4\eta/3)}, \tag{37}$$

being the quality factor due to the dissipation associated with the volume change[2]

$$Q_S=\frac{r_0/l}{KG_S}=\frac{r_0}{l}\frac{1}{K}\sqrt{\frac{\pi l c_0\rho_0}{2\eta}}, \tag{38}$$

which is the quality factor due to the dissipation associated with the shear motion in tubes.[13] Since the viscosity coeffi-

cients ζ and η are of the order of 10^{-5} and Q_S/Q_B is of the order of $\sqrt{\eta}<10^{-2}$, the overall quality factor can be approximated by Q_S, i.e.,

$$Q \simeq Q_S = \frac{r_0}{l}\frac{1}{K}\sqrt{\frac{\pi l c_0 \rho_0}{2\eta}}. \tag{39}$$

Equation (39) shows that the quality factor is proportional to ratio r_0/l and $\sqrt{l}$. The quality factors are calculated, based on Eq. (39), for four resonators used in the experiment by Lawrenson *et al.*[1] The parameters of these resonators are listed below.

Cylinder ($l=0.10$ m), $r(x)=0.0222$ m.
Cone ($l=0.17$ m), $r(x)=0.0056+0.2680x$ m.
Horn-cone ($l=0.24$ m),

$$r(x)=\begin{cases} 0.0068\cosh(23.86x), & 0\leqslant x\leqslant 0.06 \text{ m}; \\ 0.015+0.134x, & 0.06\leqslant x\leqslant 0.24 \text{ m}. \end{cases}$$

Bulb ($l=0.28$ m),

$$r(x)=\begin{cases} 0.007-0.15x+4.1x^2-9.9\times10^4x^3-9\times10^6x^4, & -0.005\,08 \text{ m}\leqslant x\leqslant 0; \\ l[0.025-0.15(x/l)+1.15(x/l)^2-0.9(x/l)^4], & 0\leqslant x\leqslant 0.28 \text{ m}. \end{cases}$$

The results are given in Table I for the resonators filled with refrigerant (R-134a).[14] The results obtained by Ilinskii *et al.*[3] are also listed in Table I, which are in a range for each resonator depending on the excitation level. It can be seen that most of quality factors are of order of 500, which was the value measured in the experiment.[1] The quality factors predicted by the present study are generally higher than the values obtained by Ilinskii *et al.*,[3] especially for the straight cylinder. This is probably due to the additional energy loss associated with turbulence generated by the large-amplitude pressures in the shaped resonators or the shock waves in the straight cylinder.

For the 2D resonator shown in Fig. 1(a), the radius expansion function is

$$f(X)=e^{\alpha X/2}, \tag{40}$$

where α is the flare constant indicating the expansion rate. The quality factors are computed for different α and the results are presented in Fig. 2. The quality factor for the 3D resonator, shown in Fig. 1(b), can be obtained by simply replacing r_0/l with h/l and setting $K=1$ in Eq. (39), which is the same for a straight cylinder. The quality factors for the 3D resonator and cylinder are also plotted in Fig. 2. It is seen, from Fig. 2, that the 2D resonators have higher quality factors than that of the 3D resonator and cylinder. This is because the energy dissipation due to the shear viscosity is reduced along the 2D resonators as the cross sections are expanded, whereas the energy dissipation in the 3D resonator is increased from the small end to the big end, as the height h between the upper/lower walls is fixed and wall areas are increased. Figure 2 also shows that the 2D resonators with larger flare numbers have higher quality factors. The difference of the quality factors between the 2D and 3D resonators affects the pressure waves in the resonators.

TABLE I. Quality factors of resonators filled with R-134a.

	Results of Ilinskii *et al.* (Ref. 3)	Results of present study	Measured value (Ref. 1)
Cylinder	350–450	1047	~500
Horn-	200–600	740	
Bulb	400–900	574	
Cone	···	745	

B. Waveforms and compression ratios

The one-dimensional wave equations (26) and (30) are solved by the Galerkin's method developed by Erickson and Zinn.[5] For comparison purposes, all parameters of the gas inside the resonators are assumed to have the same values as those used by Erickson and Zinn.[5] The coefficients of shear viscosity and bulk viscosity are of the same order, and for simplicity, we set them to be equal to $1.7E-005$ Pa·s. The resonators are oscillated at

$$A=A_0\cos(T), \tag{41}$$

and the amplitude is fixed at $A_0=5\times10^{-4}$ throughout the calculations. The cross sections of both resonators are expanded exponentially as

$$S=S_0e^{\alpha X}, \tag{42}$$

where $S_0=\pi r_0^2/l^2$ for the 2D resonator and $S_0=b_0h/l^2$ for the 3D resonator. The flare constant, α, is fixed at $\alpha=5.75$ in the following calculations because the compression ratio is the maximum at this value.[5] The dimensionless velocity potential, Φ, is expressed as

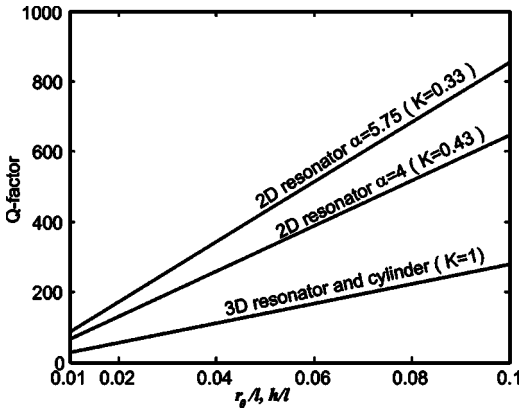

FIG. 2. The quality factor versus r_0/l and h/l for the 2D-resonator, 3D resonator, and a straight cylinder.

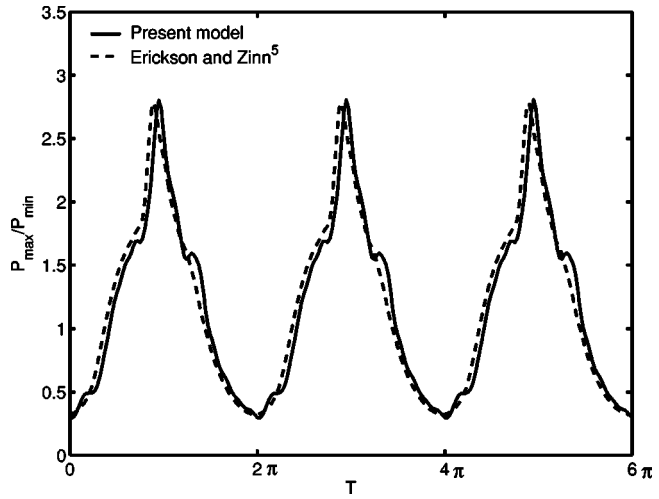

FIG. 3. Pressure waveforms at the small end of the 2D resonator. $S=\pi(r_0/l)^2e^{\alpha X}$, α=5.75. Dashed line: reproduced for the results by Erickson and Zinn (Ref. 5). Solid line: calculated from Eqs. (26) and (44), $l=0.2$ m, $r_0/l=0.023$.

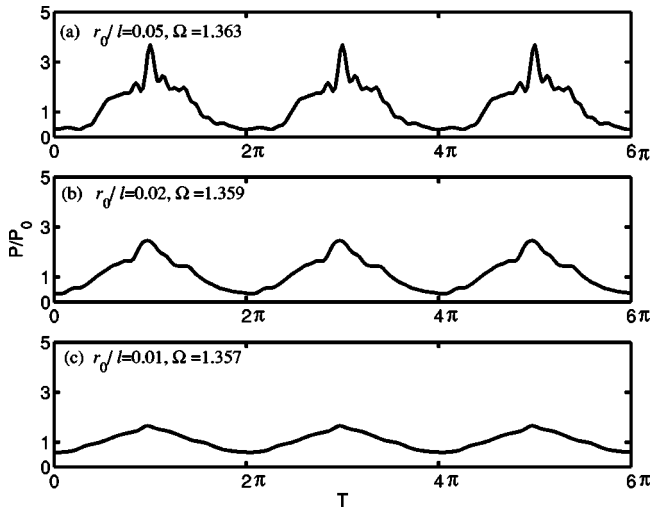

FIG. 4. Pressure waveforms at the small end of the 2D resonator. $S=\pi(r_0/l)^2e^{\alpha X}$, α=5.75, $l=0.2$ m. (a) $r_0/l=0.05$; (b) $r_0/l=0.02$; and (c) $r_0/l=0.01$.

$$\Phi(X,T)=\sum_{n=1}^{\infty}\eta_n(T)\Psi_n(X). \tag{43}$$

The trial functions, $\Psi_n(X)$, have the same forms as those used by Erickson and Zinn[5] for the resonators sealed at both ends. The time-dependent amplitudes, $\eta_n(T)$, are solved by the techniques suggested by Erickson and Zinn,[5] in which the series of Eq. (43) is truncated at $n=20$. Finally, the pressures are calculated for the 2D resonator by

$$\frac{P}{P_0}=\left[1-(\gamma-1)\pi^2\left(\Omega\frac{\partial\Phi}{\partial T}+\frac{1}{2}\left(\frac{\partial\Phi}{\partial X}\right)^2+AX-\frac{G_B}{\pi^3}\frac{1}{S}\frac{\partial}{\partial X}\left(S\frac{\partial\Phi}{\partial X}\right)+\frac{G_S\Omega^{1/2}\Phi}{R}\right)\right]^{\gamma/(\gamma-1)}, \tag{44}$$

and for the 3D resonator by

$$\frac{P}{P_0}=\left[1-(\gamma-1)\pi^2\left(\Omega\frac{\partial\Phi}{\partial T}+\frac{1}{2}\left(\frac{\partial\Phi}{\partial X}\right)^2+AX-\frac{G_B}{\pi^3}\frac{1}{S}\frac{\partial}{\partial X}\left(S\frac{\partial\Phi}{\partial X}\right)+\frac{G_S\Omega^{1/2}\Phi}{H}\right)\right]^{\gamma/(\gamma-1)}. \tag{45}$$

In Eqs. (44) and (45), P_0 is the static pressure in the resonators. As a reference, the pressure waves obtained by Erickson and Zinn[5] at the small end in the 2D resonator are reproduced here with the same condition by setting $G_S=0$ and assigning $G_B=0.01$ in Eq. (26), shown in Fig. 3 by the dashed lines. In their results (the dashed line), the pressure waveforms were not dependent on the resonator dimensions, such as the resonator length l and ratio r_0/l, because there was no shear viscosity term in the wave equation. The solid lines in Fig. 3 are the pressure waves calculated in the present study using Eqs. (26) and (44), in which G_B and G_S are evaluated according to their definitions and gas parameters, the resonator length is $l=0.2$ m, $R=r_0/l=0.023$. It is seen that two waveforms are very similar. In fact, the pressure waveforms in the resonator are dependent on the cross-section dimensions, r_0/l, due to the shear viscosity term. The resonance pressure waveforms at the small end of the 2D resonator are plotted for different values of r_0/l in Fig. 4. When r_0/l is 0.05, the pressure amplitudes are large with sharp peaks [Fig. 4(a)], indicating a strong resonance. When r_0/l is reduced to 0.02, the pressure amplitudes are reduced, as well as the sharp peaks [Fig. 4(b)]. When r_0/l is further reduced to 0.01 [Fig. 4(c)], the pressure amplitudes are reduced further and there are no sharp peaks, indicating that the resonance has been weakened due to the energy dissipation. The resonance frequency changes slightly when the ratio r_0/l varies, as denoted in the figure for each case. The similar situation is also observed for the pressure waves in the 3D resonator, which are plotted in Fig. 5. In this case, the waveforms have been smoothed down at $r_0/l=0.02$, because the 3D resonator is more dissipative than the 2D resonator, as shown by the quality factors in Fig. 3.

The compression ratios are calculated based on the

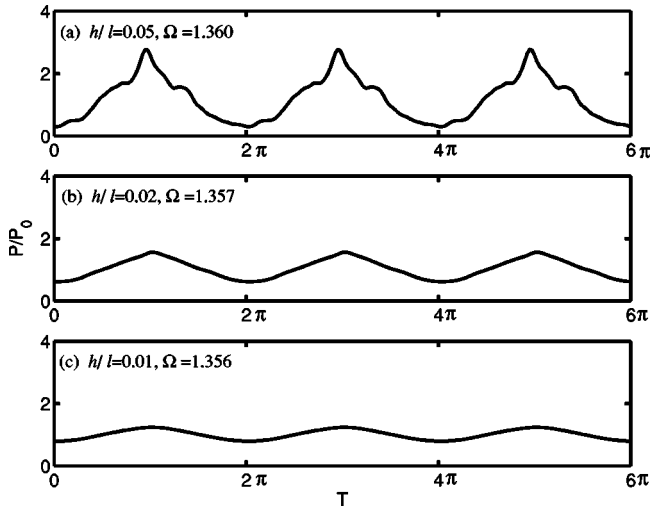

FIG. 5. Pressure waveforms at the small end of the 3D resonator. $S=b_0h/l^2e^{\alpha X}$, α=5.75, $l=0.2$ m. (a) $h/l=0.05$; (b) $h/l=0.02$; and (c) $h/l=0.01$.

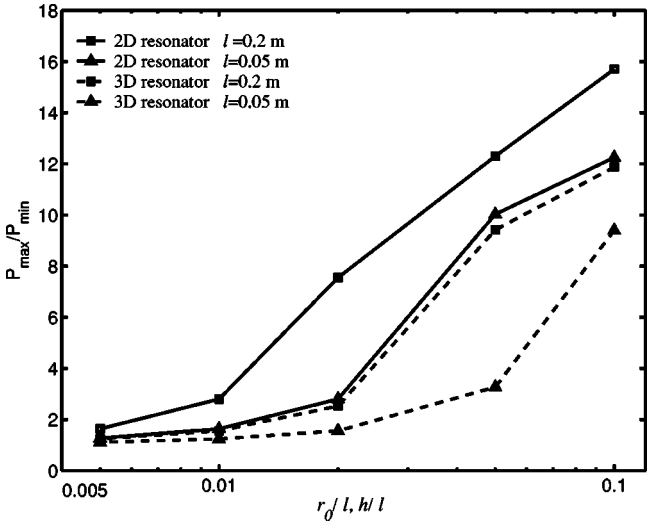

FIG. 6. Compression ratios versus r_0/l and h/l for the 2D and 3D resonators. The cross-section area is $S=\pi(r_0/l)^2e^{\alpha X}$ for the 2D resonator, and $S=hb_0/l^2e^{\alpha X}$ for the 3D resonator, $\alpha=5.75$.

maximum and minimum pressures from the waveforms, and the results for both 2D resonator and 3D resonator are presented in Fig. 6, versus r_0/l for $l=0.2$ and 0.05 m, respectively. It is seen that the compression ratios, for $l=0.2$ m, can be greater than 10 when r_0/l is greater than 0.04 for the 2D resonator and h/l is greater than 0.05 for the 3D resonator, but drop to 2 or less when r_0/l and h/l are less than 0.01, showing that the cross-section dimension of the resonator has tremendous effect on the compression ratio. On the other hand, when the overall length of the resonator is reduced, the compression ratio is also reduced, as shown in Fig. 6 by the results of $l=0.05$ m for both resonators. This is because the shorter length will lead to a higher resonance frequency, and therefore higher dissipation by the shear viscosity. It is seen from Fig. 6 that the compression ratio drops substantially at $r_0/l=0.02$ for the 2D resonator when l is reduced from 0.2 to 0.05 m, and increases quickly afterward. A similar situation is also seen for the 3D resonator but at $h/l=0.05$. The mechanism associated with these inconsistencies is not clear from the present modeling, and further study is needed. The results presented in Fig. 6 suggest that r_0/l, h/l, and l are probably the control parameters to the resonator dimensions for the given driving strength and required compression ratio. The comparison between the 2D resonator and 3D resonator in Fig. 6 shows that the compression ratios of the 3D resonator are always lower than that of 2D resonator. If one takes $l=0.05$ m and $h/l=0.05$, i.e., $l=50$ mm and $h=2.5$ mm, which is a small resonator, one may expect to have pressure waves with a compression ratio of 3, according to the results in Fig. 6. On the other hand, the resonance may be easier to be excited in a smaller resonator than in a bigger one for the same driving power. When the excitation is doubled by setting $A_0=1\times10^{-3}$ in the above-mentioned small resonator, the calculation results show that the compression ratio is increased from 3 to 10.

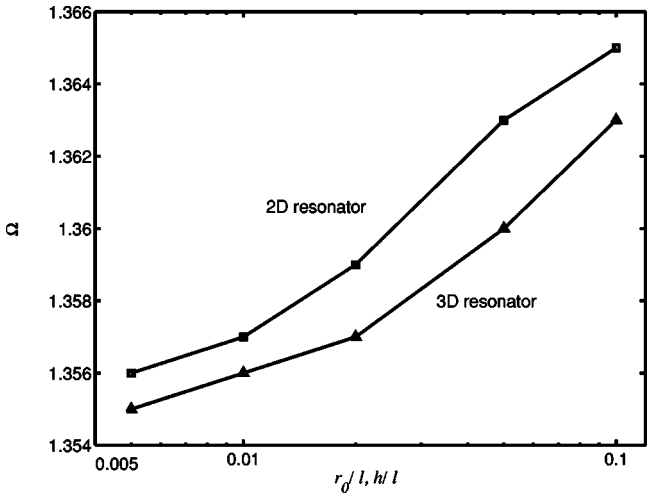

FIG. 7. Dimensionless resonance frequency versus cross-section dimensions for both 2D and 3D resonators with length $l=0.2$ m.

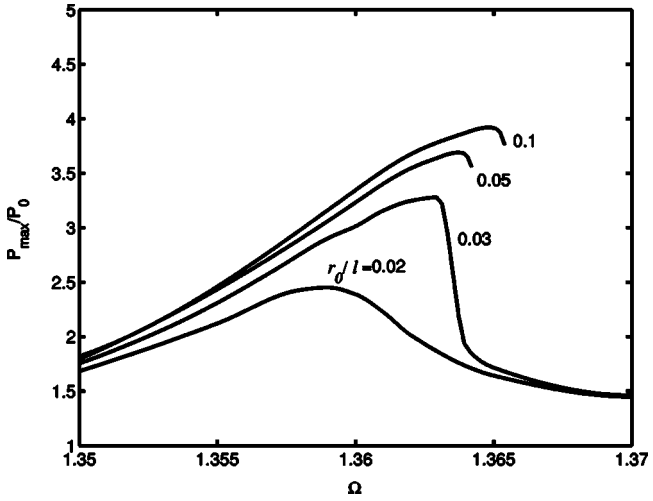

FIG. 8. Frequency response curves of the 2D resonator with different dimension ratios r_0/l. $S=\pi(r_0/l)^2e^{\alpha X}$, $\alpha=5.75$, $l=0.2$ m.

The cross-section dimensions of the resonators are found to have minor effect on the resonance frequencies, which are primarily determined by the resonator lengths and the axial-expansion shape. The calculated results for both 2D and 3D resonators, plotted out in Fig. 7, show that the variation of the dimensionless frequency (Ω) is less than 1% when the cross-section dimensions (r_0/l and h/l) change from 0.1 to 0.005. However, the changes in the resonance frequency and dimension parameters produce tremendous difference in the frequency response curves, which are illustrated in Fig. 8 by plotting the maximum pressure versus the frequency Ω for the 2D resonator. The frequency response curves at different values of parameter r_0/l in this case are very similar to the hardening behaviors of a conical resonator under different excitation levels. This resemblance indicates that the resonator dimensions affect the dynamic energy of the system through the shear viscosities.

IV. CONCLUSIONS

The effect of resonator dimensions on the nonlinear standing waves inside the shaped resonators has been studied. A shear viscosity term has been added to the one-dimensional momentum equation for the average axial veloc-

ity, and the wave equation has been solved by the Galerkin method for a 2D (axisymmetric) resonator and a 3D (low aspect ratio rectangular) resonator, whose cross sections are exponentially expanded. By calculations of quality factors, the pressure waveforms, and compression ratios, it is found that the shear viscosity dissipation plays a crucial role when the resonator sizes are reduced. The resonator length (l) and the ratio of the cross-section dimension to the length (r_0/l and h/l in the present study) are two controlling parameters. If r_0/l and h/l are greater than 0.04 for the present resonators, the typical characteristics of shaped resonators, such as high-amplitude pressures and hardening behaviors, are observed. When r_0/l and h/l are less than 0.01, the resonance becomes weak and the compression ratios drop to 2 and below, indicating that the resonators are not functioning in these cases to generate large-amplitude pressures, unless the excitation levels are increased. The results also show that the dimension ratios control the frequency response curves in the same way as the excitation level does, following the hardening behavior of the shaped resonators. Although the study is conducted based on only two specially shaped resonators, the results may be similar to other shaped resonators.

ACKNOWLEDGMENT

Luo Cheng wishes to gratefully acknowledge the scholarship from Nanyang Technological University, Singapore.

[1] C. C. Lawrenson, B. Lipkens, T. S. Lucas, D. K. Perkins, and T. W. Van Doren, ''Measurement of macrosonic standing wave in oscillating closed cavities,'' J. Acoust. Soc. Am. **104**, 623–636 (1998).

[2] Y. A. Ilinskii, B. Lipkens, T. S. Lucas, T. W. Van Doren, and E. A. Zabolotskaya, ''Nonlinear standing waves in an acoustical resonator,'' J. Acoust. Soc. Am. **104**, 2664–2674 (1998).

[3] Y. A. Ilinskii, B. Lipkens, and E. A. Zabolotskaya, ''Energy losses in an acoustical resonator,'' J. Acoust. Soc. Am. **109**, 1859–1870 (2001).

[4] M. F. Hamilton, Y. A. Ilinskii, and E. A. Zabolotskaya, ''Linear and nonlinear frequency shifts in acoustical resonator with varying cross section,'' J. Acoust. Soc. Am. **110**, 109–119 (2001).

[5] R. R. Erickson and B. T. Zinn, ''Modeling of finite amplitude acoustic wave in closed cavities using the Galerkin method,'' J. Acoust. Soc. Am. **103**, 1863–1870 (2003).

[6] N. T. Nguyen and S. T. Wereley, *Fundamentals and Applications of Microfluidics* (Artech House, 2002).

[7] M. Gad-et-Hak, ''The fluid mechanics of microdevices—The Freeman Scholar Lecture,'' J. Fluids Eng. **121**, 5–32 (1999).

[8] N. T. Nguyen and R. M. White, ''Acoustic streaming in micromachined flexural plate wave devices: numerical simulation and experimental verification,'' IEEE Trans. Ultrason. Ferroelectr. Freq. Control **47**(6), 1463–1471 (2000).

[9] D. J. Coe, M. G. Allen, M. A. Trautman, and A. Glezer, ''Micromachined Jets for Manipulation of Macroflows,'' Solid-State Sensor and Actuator Workshop, 13–16 June, Hilton Head, SC (1994).

[10] L. D. Landau and E. M. Lishitz, *Fluid Mechanics* (Pergamon, Oxford, 1987).

[11] M. Abramowitz and I. Stegun, *Handbook of Mathematical Functions with Formulas, Graphs and Mathematical Tables* (U.S. Department of Commerce, 1972).

[12] P. M. Morse and K. U. Ingard, *Theoretical Acoustics* (McGraw-Hill, New York, 1968).

[13] M. J. Moloney and D. L. Hatten, ''Acoustic quality factor and energy losses in cylindrical pipes,'' Am. J. Phys. **69**, 311–314 (2001).

[14] Japanese Association of Refrigeration, ''Thermophysical Properties of Environmentally Acceptable Fluorocarbons, HFC-134a and HCFC-123,'' (1991).